Current Optics and Photonics
Vol. 2, No. 3, June 2018, pp. 215-220

ISSN: 2508-7266(Print) / ISSN: 2508-7274(Online)
DOI: https://doi.org/10.3807/COPP.2018.2.3.215

Low Loss Highly Birefringent Porous Core Fiber for Single Mode Terahertz Wave Guidance

Md. Ahasan Habib[1]* and Md. Shamim Anower[2]

[1]Department of Electrical and Electronic Engineering, Bangabandhu Sheikh Mujibur Rahman Science & Technology University, Gopalganj 8100, Bangladesh
[2]Department of Electrical and Electronic Engineering, Rajshahi University of Engineering & Technology, Rajshahi 6204, Bangladesh

(Received March 13, 2018 : revised May 9, 2018 : accepted May 28, 2018)

A novel porous-core hexagonal lattice photonic crystal fiber (PCF) is designed and analyzed for efficient terahertz (THz) wave propagation. The finite element method based Comsol *v4.2* software is used for numerical analysis of the proposed fiber. A perfectly matched layer boundary condition is used to characterize the guiding properties. Rectangular air-holes are used inside the core to introduce asymmetry for attaining high birefringence. By intentionally rotating the rectangular air holes of porous core structure, an ultrahigh birefringence of 0.045 and low effective material loss of 0.086 cm^{-1} can be obtained at the operating frequency of 0.85 THz. Moreover, single-mode properties, power fraction in air core and confinement loss of the proposed PCF are also analyzed. This is expected to be useful for wideband imaging and telecom applications.

Keywords : Far infrared or terahertz, Fiber design and fabrication, Micro-structured fibers, Birefringence, Effective material loss
OCIS codes : (040.2235) Far infrared or terahertz; (060.2280) Fiber design and fabrication; (060.4005) Microstructured fibers; (260.1440) Birefringence

I. INTRODUCTION

Terahertz (THz) radiation band indicates the electromagnetic waves whose frequency ranges from 0.1 to 10 THz. Recently researcher’s interests have turned toward this narrow frequency band due to the promising and potential applications in the field of imaging, sensing, security, spectroscopy, oral healthcare, cancer cell detection, bio-technology, telecommunication, military and environmental applications [1-4]. The THz wave generator and detector are available in market due to the advancement of the modern technology. The THz sources are classified into three types and they are natural, artificial and THz frequency spectroscopy. Naturally, THz radiation is emitted as a part of the black-body radiation from any object when the temperature is higher than 10 K. The quantum cascade laser and backward wave oscillator (BWO) etc. are practical examples of artificial sources of THz radiation band [5, 6]. Similarly, some practical THz detectors are the thermal detector, heterodyne detection detector, direct detection detector, and field-effect transistor detector etc. On the other hand, flexible, efficient and low-loss transmission of broadband THz waves for long-length delivery remains challenging. Conventional THz systems are based on free space communications that suffer from high absorption loss due to water vapor in the surrounding atmosphere. Moreover a number of problems arise due to the misalignment between the transmitter and the receiver. To eliminate these problems, various forms of guided waveguide structures such as hollow metallic waveguides and metallic wires [7] are put in the place of unguided structure. But the common shortcoming of following waveguides is higher attenuation losses which limit the long distance communication. After

---

*Corresponding author: habib.eee.116.ah@gmail.com, ORCID 0000-0001-7732-2639

Color versions of one or more of the figures in this paper are available online.

that various forms of polymer fibers have been reported such as Bragg fiber [8], plastic fiber [9] and sub-wavelength porous fiber [10] for transmission of THz waves. But the guided medium shows high absorption in the THz regime. Then photonic crystal fiber (PCF) came into light, but the solid core of the PCFs exhibits high effective material loss (EML) [9]. In order to overcome this problem air holes are introduced in the core region thus reducing the effective material in the core region. Due to the reduced material the EML reduced drastically and this type of fiber is called porous core PCF. To significantly reduce the material loss, a larger air filling fraction (AFF) is used. Along with the low EFM another important property of porous core PCF is birefringence. Birefringence is induced in polarization-maintaining PCFs by deliberately breaking the symmetry of either core or cladding [11]. Highly birefringent THz PCFs have significant applications in optical sensing, coherent heterodyne time-domain spectrometry and measurements of biomaterials in THz frequency bands [12, 13]. For that reason a large number of researchers have proposed different structured porous core PCF. For example, Cho *et al.* [14] demonstrated a plastic PCF that exhibits a birefringence of 2.1×10^{-2} at 0.3 THz but the effective material loss is too high due to solid core. After that a hexagonal cladding and rotating hexagonal porous core PCF is proposed in [15] whose maximum birefringence is 0.033 and effective material loss (EML) of 0.43 dB/cm. The major limitations of this fiber are high effective absorption loss and fabrication difficulty. The air holes in the core are too small and are difficult to fabricate. Moreover, a special type of elliptical air hole PCF is reported in [16] which exhibits a high birefringence of 0.044 and EML of 0.42 dB/ cm. In this design elliptical air holes are used, making the design impractical because at the time of fabrication it is very difficult to maintain two different axes of a single air hole. Recently a diamond shaped porous core PCF is proposed by Islam *et al.* which exhibits low birefringence of 0.017 and EML 0f 0.11 for optimal design parameters at 1 THz [17]. The design of this fiber is very simple and easy to realize but the EML is very high.

In this paper a simple hexagonal lattice PCF is proposed in which rectangular shaped air holes are introduced in the core region. The air holes of the core are rotated to get high birefringence and at optimum designing condition the proposed fiber shows simultaneously a high-birefringence of 0.045 and a low effective absorption loss of 0.086 cm^{-1}. Moreover the other guiding properties such as confinement loss, bending loss, power fraction and single mode propagation are discussed rigorously.

II. DESIGN METHODOLOGY

The cross section of the proposed porous core PCF is reported in Fig. 1. In the cladding region a hexagonal shaped structure with three rings is chosen. This type of structure is chosen due to four main reasons. They are (i) the hexagonal structure provides better confinement of light, (ii) only one pitch (distance between two adjacent air holes, Λ) is used in the cladding which make fabrication easy, (iii) high air filling fraction (AFF) makes the design compact and (iv) the fewer air hole rings make the fiber thicker which is important for the flexibility of the fiber.

The diameter of the cladding air hole is denoted by d. The air-filling ratio (d/Λ) of the cladding is 0.95 and it remains constant throughout the analysis. In the proposed design rectangular type air holes are introduced in the core. The height and width of the rectangular air holes are related to Λ. The distance between two air holes in same column is l_c and distance between two column is l_r which are $l_c = 0.13*\Lambda$ and $l_r = 0.065*\Lambda$ respectively and they are kept constant throughout the simulation. The prime reason for selecting these particular values is that, it ensures lowest EML without overlapping the air holes and maximum birefringence has been found for that particular value. The background material considered for this design is cyclic-olefin copolymer (COC), with a trade name of TOPAS. This polymer is preferred due to some of its excellent merits over other polymers such as PMMA or Teflon. For example, its refractive index is constant n = 1.5258 between 0.1~2 THz [17], its effective material loss is 0.2 cm^{-1} at 1 THz which is lower compared to other polymers. A circular perfectly matched layer (PML) boundary condition is used whose thickness is 15% of the total radius of the fiber.

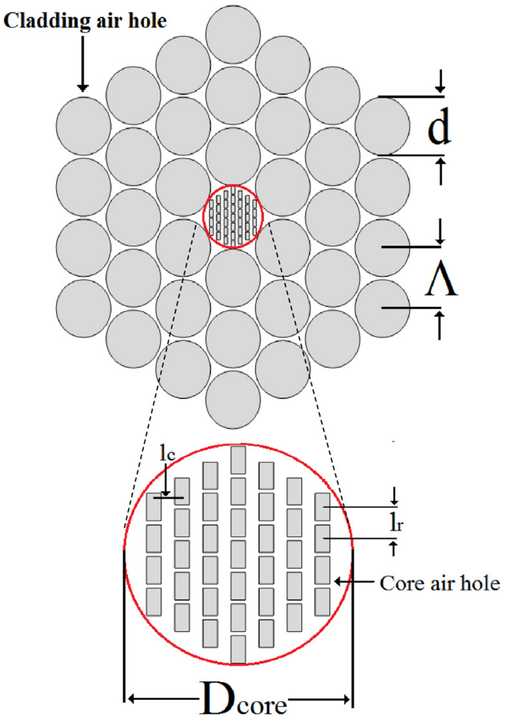

FIG. 1. The cross-sectional view of the proposed PC-PCF.

III. SIMULATION RESULTS AND DISCUSSION

The finite element method (FEM) based *Comsol v.4.2* software has been used to design and investigate the properties of the proposed porous core PCF. A circular PML boundary condition is considered outside of the cladding to absorb the electromagnetic field which will propagate towards the surface of the fiber. For the efficient transmission of THz wave, the electromagnetic field should be tightly confined in the core region. Figure 2 indicates the mode field distribution of the proposed fiber and from the figure it is clear that the light is tightly confined in the core region.

To operate as an effective polarization-maintaining THz PCF, the level of birefringence should be as high as possible. The birefringence has been calculated using the following formula [17]

$$B = |n_x - n_y| \tag{1}$$

where B is the birefringence, n_x and n_y are the refractive indices of x- polarization and y- polarization respectively. The birefringence as a function of frequency at different rotation angle is shown in Fig. 3 and it is seen that the birefringence is good at 0 and 60 degree rotation at $D_{core} =$ 375 μm. For maximum birefringence 60° rotated air holes fiber is considered as optimum designing condition. The birefringence is as high as 0.045 and this is higher than the previous reported work [14-17].

When a light wave of more than one mode propagates through the core then the fiber is subjected to modal distortion. In order to get rid of modal distortion single mode fiber can be used. The single mode condition of any porous core fiber can be calculated by using the following expression

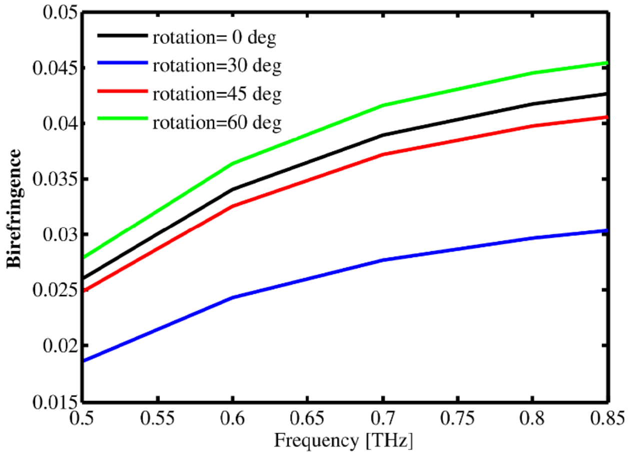

FIG. 3. Birefringence as a function of frequency for 375 μm core diameter.

$$V_{eff} = \frac{2\pi r f}{c}\sqrt{n_{co}^2 - n_{cl}^2} \tag{2}$$

where V_{eff} is called the normalized frequency, c is the velocity of the light in free space, r is the radius of the fiber core, f is the frequency of the wave propagating through the PCF, n_{co} and n_{cl} are the effective refractive index of the core and cladding region respectively. The condition for single mode propagation is $V_{eff} \leq 2.405$. The V parameter is calculated for this optimum condition only. Figure 4 shows the single mode properties of the proposed fiber and it is clear that the value of V_{eff} is lower than 2.405 which indicates that this fiber will not create modal distortion when a light wave propagates through it.

When light wave propagates through the PCF then due to the property of the fiber material the signal is attenuated. Designing a low loss fiber is a major challenge for the

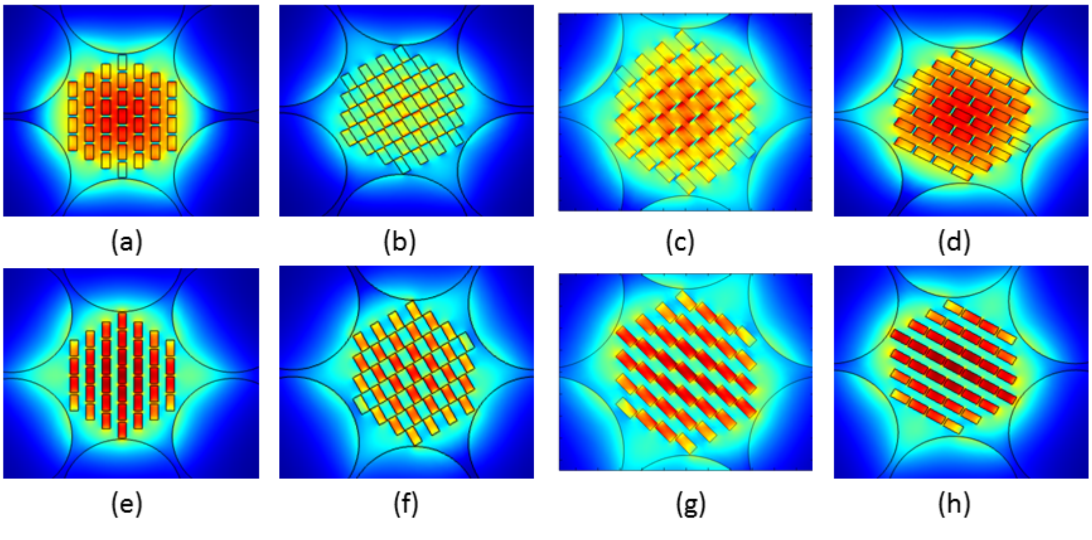
(a) (b) (c) (d)
(e) (f) (g) (h)

FIG. 2. Mode field distribution of the proposed PCF for core diameter 375 μm and 0.85 THz operating frequencies for (a) 0°, x-pol (b) 30°, x-pol (c) 45°, x-pol (d) 60°, x-pol (e) 0°, y-pol (f) 30°, y-pol (g) 45°, y-pol (h) 60°, y-pol.

scientists in this field. The major loss mechanism, material absorption loss or effective material loss (EML) is quantified by the following expression [17]

$$\alpha_{eff} = \frac{\left(\varepsilon_0 / \mu_0 \right)^{1/2} \int_{A_{mat}} n\, \alpha_{mat} \left| \mathrm{E} \right|^2 dA}{2 \int_{All} S_z dA} \ \mathrm{cm}^{-1} \tag{3}$$

where ε_0 and μ_0 are the permittivity and permeability of the vacuum, n is the refractive index of the material used, E is the modal electric field, α_{mat} is the bulk material absorption loss and S_z is the z-component of the Poynting vector. Figure 5 shows the variation of effective material loss as a function of core diameter. It is seen from Fig. 5 that the increment of core diameter causes the effective material loss to increase. Moreover, fiber thickness is also an important parameter for the THz application and its flexibility. In order to be flexible and for compactness the fiber should be as thin as possible [15]. Therefore, we have chosen 375 μm as optimum core diameter. The effective material loss of the proposed fiber is also lower than the previous reported work in [14-17]. Again the EML of the proposed fiber for different operating frequencies at 375 μm core diameter is shown in Fig. 6. From Fig. 6 it is seen that the EML is very low over a wide range of frequency of 0.5~0.85 THz. So, this fiber may be applicable in any type of long distance communication.

Another kind of loss mechanism occurs in a photonic crystal fiber is known as confinement loss. Confinement loss is an important guiding property because it limits the length of the THz transmission system which is obtained from the imaginary part of the complex refractive index, n_{eff} is given by [15]

$$\alpha_{CL} = 8.686 \times \frac{2\pi f}{c} \mathrm{Im}(n_{eff}) \times 10^{-2} \ \mathrm{dB/cm} \tag{4}$$

where f is the frequency of the light, c is the speed of the light in vacuum and $\mathrm{Im}(n_{eff})$ is the imaginary part of the refractive index of the guided mode. Figure 7 shows the

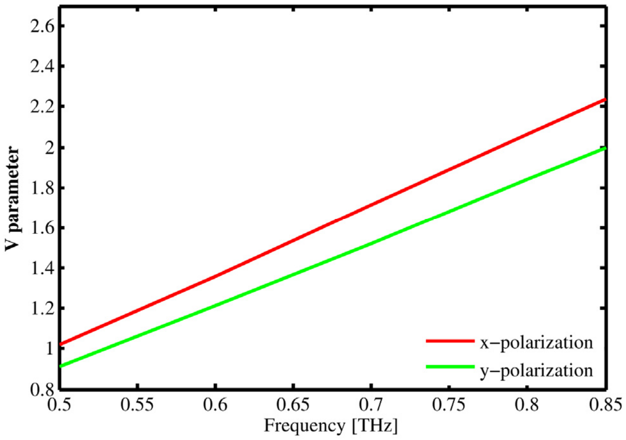

FIG. 4. V- parameter as a function of frequency at optimal rotation angle 60° for x and y polarization.

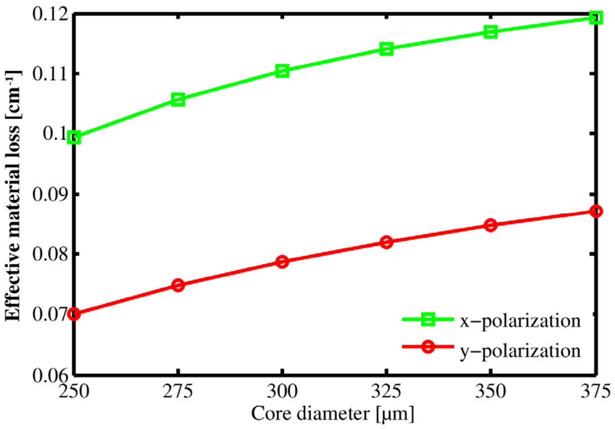

FIG. 5. EML as a function of core diameter for 60° rotation at 0.85 THz.

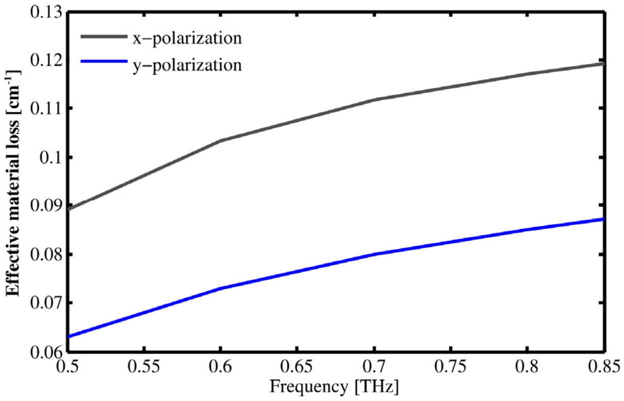

FIG. 6. EML as a function of frequency for 60° rotation and 375 μm core diameter.

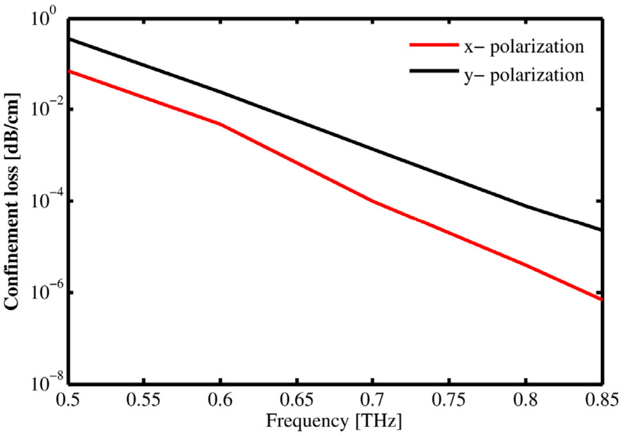

FIG. 7. Confinement loss as a function of frequency for 60° rotation and 375 μm core diameter.

variation of confinement loss as a function of frequency. The confinement loss decreases with the increase of core diameter at a particular frequency because the increased core diameter provides more space and it is lower than Refs. [14-17].

And now it is expected that the light is well confined in the core and if so, most of the light should pass through the core air holes in the case of porous core fibers. How much power is propagating in the air core can be quantified by the term called power fraction, which is expressed by

$$\eta = \frac{\int_X S_z dA}{\int_{All} S_z dA} \tag{5}$$

where η represents the mode power fraction and X is the region of interest through which the power is to be calculated. The mode fraction power is reported in Fig. 8 and the figure represents that almost 37.24% of the total power travels through the core air holes and it is better than previous work in [14, 15]. The amount of power through the core is not reported in [17].

For realizing a PCF in practical applications bending loss analysis is very important. To calculate the bending loss, at first the bent fiber is replaced by its equivalent straight fiber. Then the effective refractive index of that fiber is found from the conformal transformation method which is used to calculate the leakage loss. The bending loss can be calculated by using the following equation [17]

$$\alpha_{BL} = \frac{1}{8}\sqrt{\frac{2\pi}{3}}\frac{1}{A_{eff}}\frac{1}{\beta}F\left[\frac{2}{3}R\frac{\left(\beta^2-\beta_{cl}^2\right)^{3/2}}{\beta^2}\right] \tag{6}$$

where R is the bending radius, $F(x) = x^{-1/2}e^{-x}$, the propagation constant β and β_{cl} are defined as $\beta = 2\pi n_{co} / \lambda$ and $\beta_{cl} = 2\pi n_{cl} / \lambda$. And A_{eff} is the effective area. The bending loss of the proposed fiber is shown in Fig. 9 and the following figure shows that the bending loss decreases with the increase of the frequency. The bending loss is not shown in [14-17].

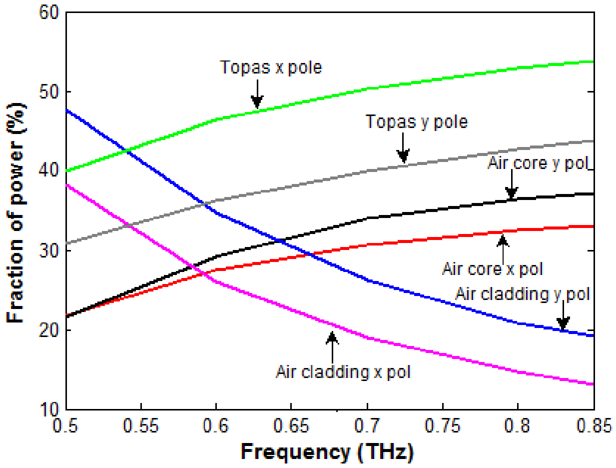

FIG. 8. Power fraction as a function of frequency at D_{core} = 375 µm.

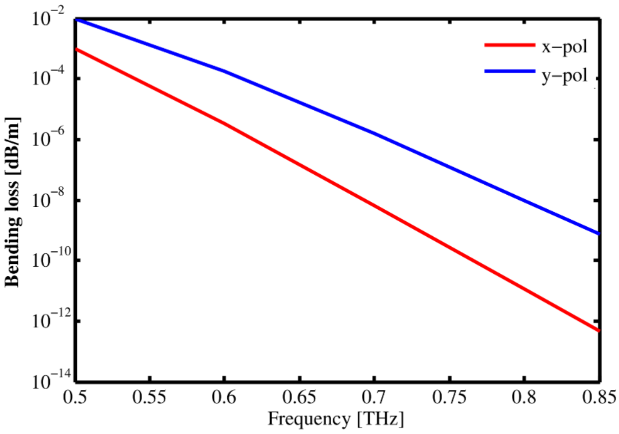

FIG. 9. Bending loss as a function of frequency of the proposed fiber for optimal condition.

Now, the comparison among some previous paper and the proposed design is shown in Table 1.

IV. CONCLUSION

An efficient slotted-core PCF has been analyzed and demonstrated for polarization maintaining applications. The

TABLE 1. Comparison of this PC-PCF with some previously remarkable designs

Type of PCF	Birefringence	EML [cm^{-1}]	Confinement loss [dB/cm]	Bending loss [dB/m]	Core power fraction [%]
Ref [14]	0.021	0.10	-	-	-
Ref [15]	0.033	0.1008	-	-	31
Ref [16]	0.044	0.1008	-	-	36
Ref [17]	0.017	0.11	> 0.1	> 10	-
Our PC-PCF	0.045	0.086	< 10^{-6}	0.83 × 10^{-10}	37.24

proposed model presents extremely high birefringence of 0.045 and a very low effective material loss of 0.086 cm^{-1} at 0.85 THz operating frequency. The structure is expected to be fabricated using the ongoing fabrication technology combining the extrusion techniques [18]. The proposed structure is compact and robust and it would be an efficient guiding structure for THz wave transmission.

REFERENCES

1. M. M. Awad and R. A. Cheville, "Transmission terahertz waveguide-based imaging below the diffraction limit," Appl. Phys. Lett. **86**, 221107-1-221107-3 (2005).
2. R. M. Woodward, V. P. Wallace, D. D. Arnone, E. H. Linfield, and M. J. Pepper, "Terahertz pulsed imaging of skin cancer in the time and frequency domain," Biol. Phys. **29**, 257-259 (2003).
3. A. Y. Pawar, D. D. Sonawane, K. B. Erande, and D. V. Derle, "Terahertz technology and its applications," Drug Invent. Today **5**, 157-163 (2013).
4. M. R. Hasan, M. S. Anower, M. A. Islam, and S. M. A. Razzak, "Polarization-maintaining low-loss porous-core spiral photonic crystal fiber for terahertz wave guidance," Appl. Opt. **55**, 4145-4152 (2016).
5. S. Fathololoumi, E. Dupont, C. W. I. Chan, Z. R. Wasilewski, S. R. Laframboise, D. Ban, A. Mátyás, C. Jirauschek, Q. Hu, and H. C. Liu, "Terahertz quantum cascade lasers operating up to ~200 K with optimized oscillator strength and improved injection tunneling," Opt. Express **20**, 3866 (2012).
6. A. W. M. Lee, Q. Qin, S. Kumar, B. S. Williams, and Q. Hu, "Real-time terahertz imaging over a standoff distance (> 25 meters)," Appl. Phy. Lett. **89**, 141125(1-3) (2006).
7. K. Wang and D. M. Mittleman, "Metal wires for terahertz wave guiding," Nature **432**, 376-379 (2004).
8. A. Dupuis, K. Stoeffler, B. Ung, C. Dubois, and M. J. Skorobogatiy, "Hollow-core terahertz optical waveguides with hyperuniform disordered reflectors," Opt. Soc. Am. B **28**, 896-907 (2011).
9. H. Han, H. Park, M. Cho, and J. Kim, "Terahertz pulse propagation in a plastic fiber," Appl. Phys. Lett. **80**, 2634-2639 (2002).
10. L. J. Chen, H. W. Chen, T. F. Kao, J. Y. Lu, and C. K. Sun, "Low-loss subwavelength plastic fiber for terahertz waveguiding," Opt. Lett. **31**, 308-310 (2006).
11. S. E. Kim, B. H. Kim, C. G. Lee, S. Lee, K. Oh, and C. S. Kee, "Elliptical defected core photonic crystal fiber with high birefringence and negative flattened dispersion," Opt. Express **20**, 1385-1391 (2012).
12. J. Noda, K. Okamoto, and Y. Sasaki, "Polarization-maintaining fibers and their applications," J. Lightw. Technol. **4**, 1071-1089 (1986).
13. M. B. Byrne, M. U. Shaukat, J. E. Cunningham, E. H. Linfield, and A. G. Davies, "Low-loss and bend-insensitive terahertz fiber using a rhombic shaped core," Appl. Phys. Lett. **98**, 151104 (2011).
14. M. Cho, J. Kim, H. Park, Y. Han, K. Moon, E. Jung, and H. Han, "Highly birefringent terahertz polarization maintaining plastic photonic crystal fibers," Opt. Express **16**, 712 (2008).
15. G. K. M. Hasanuzzaman, S. Rana, and M. S. Habib, "A novel low loss, highly birefringent photonic crystal fiber in THz regime," IEEE Photon. Technol. Lett. **28**, 899-902 (2016).
16. N. Chen, J. Liangand, and L. Ren, "High-birefringence, low-loss porous fiber for single-mode terahertz wave guidance," Appl. Opt. **52**, 5297-5302 (2013).
17. R. Islam, M. S. Habib, G. K. M. Hasanuzzaman, S. Rana, M. A. Sadat, and C. Markos, "A novel low loss diamond-core porous fiber for polarization maintaining terahertz transmission," IEEE Photon. Technol. Lett. **28**, 1537-1540 (2016).
18. K. M. Kiang, K. Frampton, T. M. Monro, R. Moore, J. Tucknott, D. W. Hewak, D. J. Richardson, and H. N. Rutt, "Extruded singlemode non-silica glass holey optical fibres," Electron. Lett. **38**, 546-547 (2002).